A Cdc20-APC Ubiquitin Signaling Pathway Regulates Presynaptic Differentiation

Yue Yang,[1,2] Albert H. Kim,[1,3] Tomoko Yamada,[1] Bei Wu,[4] Parizad M. Bilimoria,[1,2] Yoshiho Ikeuchi,[1] Núria de la Iglesia,[1] Jie Shen,[2,4] Azad Bonni[1,2]*

Presynaptic axonal differentiation is essential for synapse formation and the establishment of neuronal circuits. However, the mechanisms that coordinate presynaptic development in the brain are largely unknown. We found that the major mitotic E3 ubiquitin ligase Cdc20-anaphase promoting complex (Cdc20-APC) regulates presynaptic differentiation in primary postmitotic mammalian neurons and in the rat cerebellar cortex. Cdc20-APC triggered the degradation of the transcription factor NeuroD2 and thereby promoted presynaptic differentiation. The NeuroD2 target gene encoding Complexin II, which acts locally at presynaptic sites, mediated the ability of NeuroD2 to suppress presynaptic differentiation. Thus, our findings define a Cdc20-APC ubiquitin signaling pathway that governs presynaptic development, which holds important implications for neuronal connectivity and plasticity in the brain.

The establishment of neuronal circuitry during brain development requires the formation of synapses between neurons, and an essential part of this is presynaptic axon differentiation. Synapse development is regulated by the ubiquitin-proteasome pathway (*1*, *2*). However, an E3 ubiquitin ligase that orchestrates presynaptic differentiation in the mammalian brain remained to be identified.

The cell cycle–regulated ubiquitin ligase, the anaphase-promoting complex (APC), is highly expressed in postmitotic mammalian neurons (fig. S1A) (*3*, *4*). The APC associates with the critical coactivator Cdc20 or Cdh1 (*3*, *4*). Although Cdh1-APC controls axon growth and patterning (*3*), it does not appear to regulate the number of presynaptic sites in rat cerebellar granule neurons (fig. S13). We thus asked whether Cdc20-APC plays a role in presynaptic differentiation.

To study presynaptic development, we first characterized clustering of the synaptic vesicle protein

[1]Department of Pathology, Harvard Medical School, Boston, MA 02115, USA. [2]Program in Neuroscience, Harvard Medical School, Boston, MA 02115, USA. [3]Department of Neurosurgery, Brigham and Women's Hospital, Boston, MA 02115, USA. [4]Center for Neurologic Diseases, Brigham and Women's Hospital, Boston, MA 02115, USA.

*To whom correspondence should be addressed. E-mail: azad_bonni@hms.harvard.edu

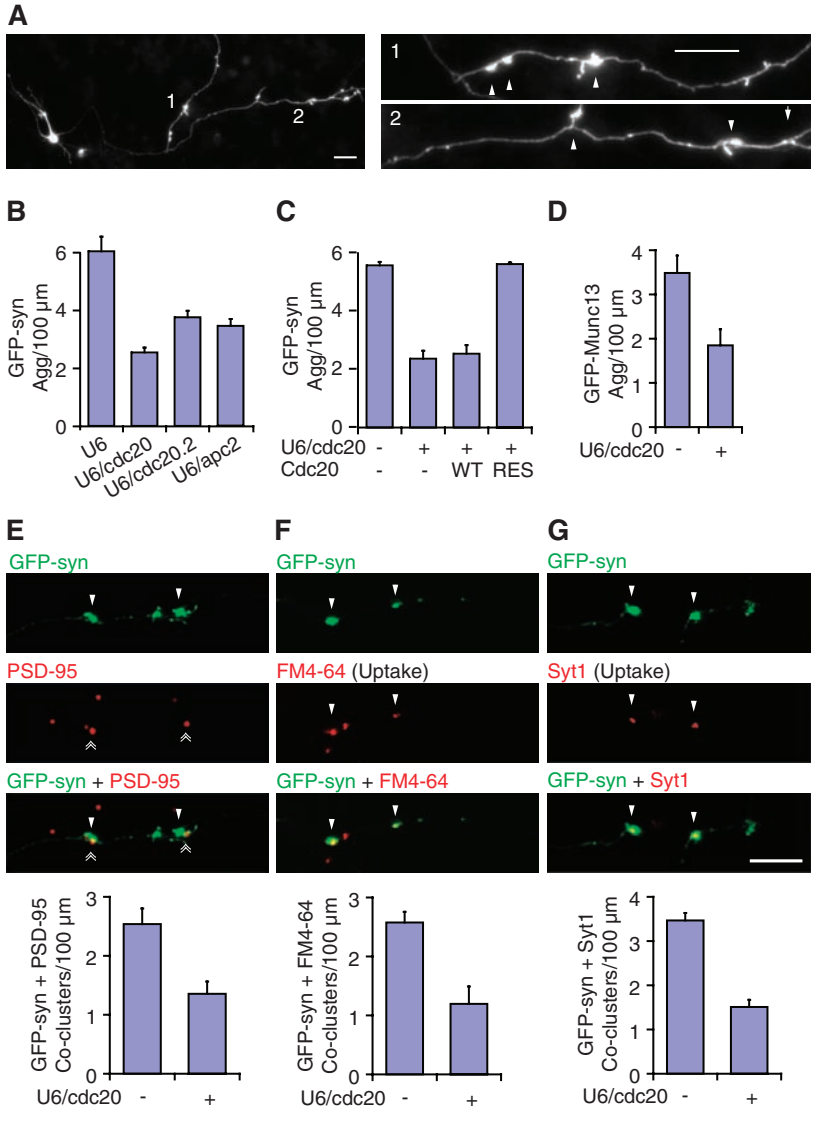

Fig. 1. Cdc20-APC induces presynaptic differentiation in postmitotic neurons. (**A**) Image of a cerebellar granule neuron transfected with a GFP-synapsin expression plasmid. Distal axons are shown in right panels. Arrowheads denote synapsin clusters. (**B**) Knockdown of Cdc20 (U6/cdc20 or U6/cdc20.2) or APC2 (U6/apc2) decreased synapsin cluster density in granule neurons [$P < 0.01$, analysis of variance (ANOVA) followed by Fisher's protected least significant difference (PLSD) post hoc test, $n = 3$]. (**C**) Expression of Cdc20-RES, but not Cdc20-WT, increased synapsin clustering in the background of Cdc20 RNAi ($P < 0.001$, ANOVA followed by Fisher's PLSD post hoc test, $n = 3$). (**D**) Cdc20 knockdown decreased Munc13 clusters ($P < 0.01$, t test, $n = 3$). (**E**) (Top) granule neurons expressing GFP-synapsin were subjected to immunocytochemistry using GFP and PSD-95 antibodies. Arrowheads indicate representative synapsin/PSD-95 coclusters. (Bottom) Cdc20 knockdown reduced the density of synapsin/PSD-95 coclusters ($P < 0.05$, t test, $n = 3$). (**F** and **G**) (Top) Granule neurons expressing GFP-synapsin were analyzed for synaptic vesicle recycling using the uptake of the dye FM4-64 or a luminal Syt1 antibody. Arrowheads indicate representative synapsin and FM4-64 or Syt1 coclusters. (Bottom) Cdc20 knockdown reduced the density of synapsin coclustered with FM4-64 ($P < 0.05$, t test, $n = 3$) or Syt1 ($P < 0.001$, t test, $n = 3$) uptake sites. Scale bars, 20 µm.

synapsin in primary granule neurons isolated from the rat cerebellar cortex. To visualize synapsin clustering, we transfected granule neurons with an expression plasmid encoding synapsin fused to green fluorescent protein (GFP-synapsin) (*5*). We observed GFP-synapsin clusters preferentially in the distal portion of axons, and these clusters overlapped with the endogenous synaptic vesicle proteins VAMP2 and VGlut1 (Fig. 1A and fig. S1, B to D).

To determine the role of Cdc20-APC in synapsin clustering, we induced knockdown of Cdc20 in neurons using two independent short hairpin RNAs (shRNAs) (fig. S2A) (*4*). Synapsin clustering was robustly reduced in Cdc20 knockdown neurons (Fig. 1B and fig. S2B). Expression of a rescue form of Cdc20 encoded by an RNA interference (RNAi)–resistant cDNA (Cdc20-RES), but not Cdc20 encoded by wild-type cDNA (Cdc20-WT), reversed the Cdc20 RNAi-induced loss of synapsin clusters in neurons, suggesting that the Cdc20 RNAi-induced phenotype is the result of specific knockdown of Cdc20 in neurons (Fig. 1C and fig. S2C) (*4*). Cdc20 knockdown in cerebellar slices also reduced synapsin cluster density in granule neuron parallel fiber axons (fig. S3). In other experiments, knockdown of the core APC subunit APC2 in granule neurons reduced the density of synapsin clusters (Fig. 1B and fig. S2, A and B). Together, these results suggest that Cdc20-APC drives synapsin clustering in postmitotic neurons.

We asked whether Cdc20-APC regulates other aspects of presynaptic differentiation. GFP-synapsin clusters colocalized with clusters of endogenous active zone proteins, including Munc13, Bassoon, Rim1, and Liprin-alpha (fig. S4A). Accordingly, knockdown of Cdc20 triggered the loss of GFP-Munc13 clusters along the axon in granule neurons (Fig. 1D and fig. S4B). Thus, Cdc20-APC promotes the coordinate clustering of synaptic vesicle and active zone proteins.

We next assessed whether Cdc20-APC promotes the differentiation of functional presynaptic sites that form synapses. Synapsin clusters were apposed to clusters of the postsynaptic protein PSD-95, and Cdc20 knockdown reduced the density of synapsin/PSD-95 coclusters in granule neurons (Fig. 1E). In other experiments in which we measured the ability of axons to undergo synaptic vesicle recycling, synapsin clusters were found to be colocalized with sites of uptake of the dye FM4-64 or a luminal Syt1 antibody (*6*, *7*), and Cdc20 knockdown reduced the density of synapsin coclusters with FM4-64 or Syt1 uptake sites (Fig. 1, F and G). Collectively, our results suggest that Cdc20-APC drives the differentiation of presynaptic sites that are functionally active and that form synapses.

Because the ubiquitin ligase activity of Cdc20-APC is critical for its function, we reasoned that neuronal Cdc20-APC promotes presynaptic differentiation by inducing the degradation of a protein that inhibits presynaptic development. The brain-enriched transcription factor NeuroD2 harbors the Cdc20 recognition motif, the destruction box (D-box) (*8*), suggesting that NeuroD2 might be a target of Cdc20-APC in the control of presynaptic development. NeuroD2 protein levels decreased in the developing rat cerebellum and in primary granule neurons with maturation, inversely correlating with the increasing levels of Cdc20 (Fig. 2A and fig. S5, A and B). Endogenous NeuroD2 levels increased in granule neurons treated with the proteasome inhibitor MG132 (Fig. 2B). In other experiments, NeuroD2 was found to be conjugated with ubiquitin in neurons (Fig. 2C). Together, these results suggest that NeuroD2 is regulated by the ubiquitin-proteasome system.

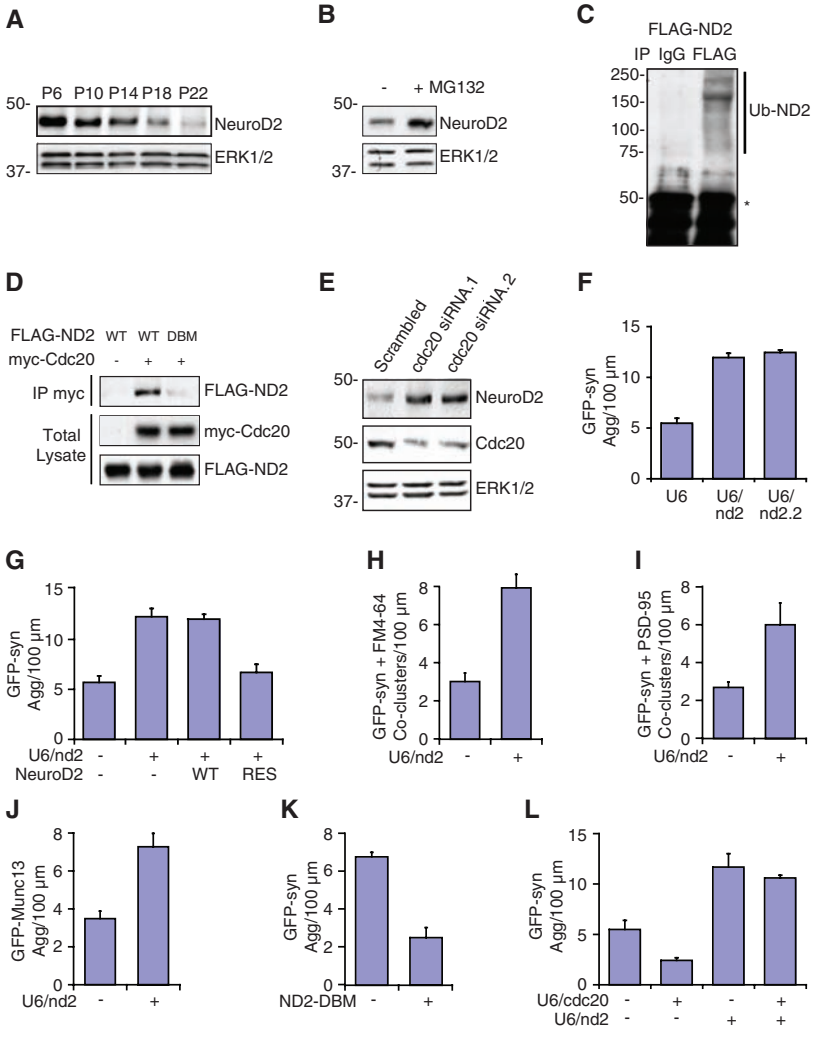

Fig. 2. Cdc20-APC–induced degradation of NeuroD2 drives presynaptic differentiation. (**A**) Lysates of cerebella from rat pups at postnatal days 6, 10, 14, 18, and 22 were immunoblotted with antibody to NeuroD2 or extracellular signal–regulated kinase 1/2 (ERK1/2). (**B**) Lysates of granule neurons treated with MG132 (5 μM) or vehicle were immunoblotted with the NeuroD2 or ERK1/2 antibody. (**C**) Lysates of granule neurons transfected with the FLAG-NeuroD2 expression plasmid were immunoprecipitated with the FLAG antibody or control immunoglobulin G followed by immunoblotting with the ubiquitin antibody. (**D**) Lysates of 293T cells transfected with the FLAG-ND2-WT or FLAG-ND2-DBM expression plasmid together with the myc-Cdc20 expression plasmid or its control vector were immunoprecipitated with the myc antibody followed by immunoblotting with the FLAG antibody. Total lysates were immunoblotted with the myc or FLAG antibody. (**E**) Lysates of granule neurons transfected with two different small interfering RNAs (siRNAs) targeting Cdc20 or a scrambled control siRNA were immunoblotted with the NeuroD2, Cdc20, or ERK1/2 antibody. (**F**) Knockdown of NeuroD2 by two different shRNAs (U6/nd2 or U6/nd2.2) in granule neurons led to a greater than 100% increase in synapsin cluster density ($P < 0.001$, ANOVA followed by Fisher's PLSD post hoc test, $n = 3$). (**G**) Expression of NeuroD2-RES, but not NeuroD2-WT, suppressed synapsin clustering in the background of NeuroD2 RNAi ($P < 0.001$, ANOVA followed by Fisher's PLSD post hoc test, $n = 3$). (**H** and **I**) NeuroD2 knockdown increased the density of synapsin/FM4-64 ($P < 0.01$, t test, $n = 3$) and synapsin/PSD-95 ($P < 0.05$, t test, $n = 3$) coclusters. (**J**) NeuroD2 knockdown increased the density of Munc13 clusters ($P < 0.001$, t test, $n = 3$). (**K**) Expression of ND2-DBM suppressed synapsin clustering ($P < 0.01$, t test, $n = 3$). (**L**) Knockdown of Cdc20 reduced synapsin clustering ($P < 0.05$, ANOVA followed by Fisher's PLSD post hoc test, $n = 3$), but did not reduce synapsin clustering in the background of NeuroD2 RNAi.

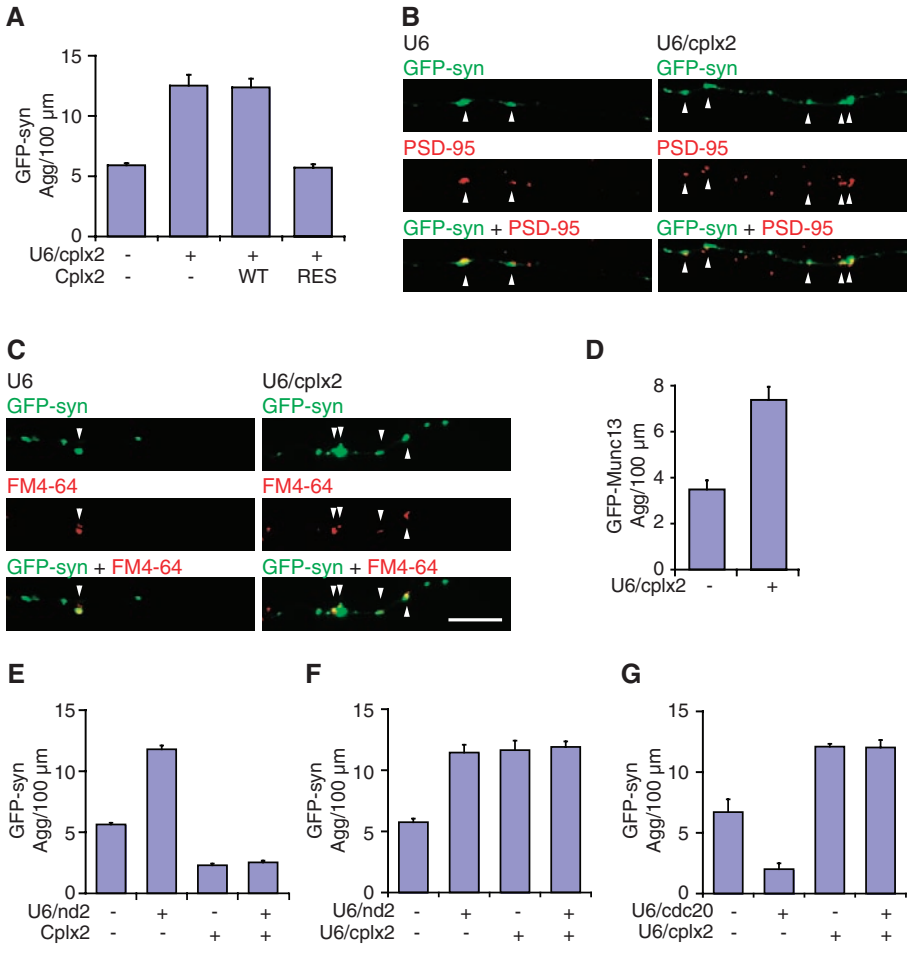

Fig. 3. The NeuroD2 target gene, Complexin II, inhibits presynaptic differentiation. (**A**) Granule neurons were transfected with the GFP-synapsin expression plasmid together with the control U6 or U6/cplx2 RNAi plasmid and an expression plasmid encoding Cplx2-WT, Cplx2-RES, or a control vector. Cplx2 knockdown increased synapsin clustering, and expression of Cplx2-RES but not Cplx2-WT reduced synapsin cluster density in the background of Cplx2 RNAi ($P < 0.01$, ANOVA followed by Fisher's PLSD post hoc test, $n = 3$). (**B** and **C**) Cplx2 knockdown increased the density of synapsin/PSD-95 and synapsin/FM4-64 coclusters. For quantification, see fig. S8, C and D. (**D**) Cplx2 knockdown induced Munc13 clustering ($P < 0.001$, t test, $n = 3$). (**E**) Expression of exogenous Cplx2 suppressed the NeuroD2 RNAi-induced increase in synapsin clustering ($P < 0.001$, ANOVA followed by Fisher's PLSD post hoc test, $n = 3$). (**F**) Simultaneous knockdown of Cplx2 and NeuroD2 did not increase synapsin density to a greater extent than with knockdown of each gene alone. (**G**) Knockdown of Cplx2 reversed the Cdc20 RNAi-induced loss of synapsin clusters ($P < 0.001$, ANOVA followed by Fisher's PLSD post hoc test, $n = 3$). Scale bars, 20 μm.

We assessed the role of Cdc20-APC in the regulation of NeuroD2 protein abundance in neurons. NeuroD2 formed a physical complex with Cdc20 in cells, but a NeuroD2 protein in which the D-box was mutated (ND2-DBM) failed to associate with Cdc20 (Fig. 2D and fig. S5C). Endogenous NeuroD2 levels increased upon Cdc20 knockdown in neurons (Fig. 2E). Thus, Cdc20-APC controls the abundance of NeuroD2 protein in neurons.

The identification of NeuroD2 as a target of Cdc20-APC in neurons would predict that NeuroD2 suppresses synapsin clustering. Consistent with this prediction, NeuroD2 knockdown increased the density of synapsin clusters in granule neurons by a factor of more than two (Fig. 2F and fig. S5, D and E). Expression of an RNAi-resistant rescue form of NeuroD2 (NeuroD2-RES), but not NeuroD2-WT, reversed the NeuroD2 RNAi-induced increase in synapsin cluster density in neurons (Fig. 2G and fig. S5F). NeuroD2 knockdown also increased synapsin cluster density in parallel fiber axons in cerebellar slices (fig. S6A). In other experiments, NeuroD2 knockdown in granule neurons increased the density of synapsin/FM4-64 and synapsin/Syt1 coclusters by a factor of more than two (Fig. 2H and fig. S6, B to D). Further, the NeuroD2 knockdown-induced synapsin clusters were apposed to PSD-95 (Fig. 2I and fig. S6E). NeuroD2 knockdown also increased clustering of the active zone protein Munc13 in

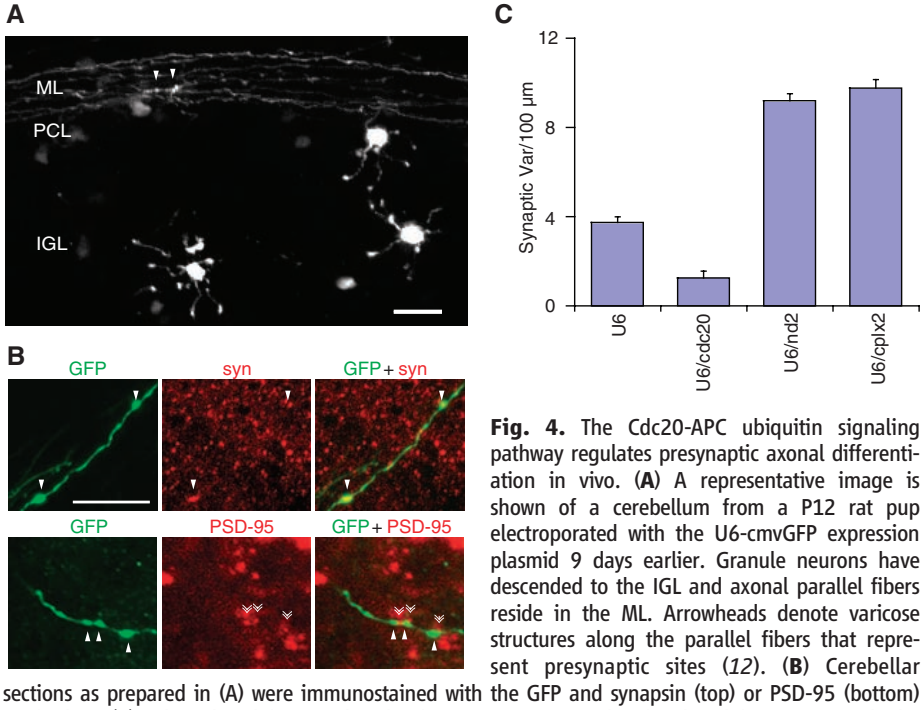

Fig. 4. The Cdc20-APC ubiquitin signaling pathway regulates presynaptic axonal differentiation in vivo. (**A**) A representative image is shown of a cerebellum from a P12 rat pup electroporated with the U6-cmvGFP expression plasmid 9 days earlier. Granule neurons have descended to the IGL and axonal parallel fibers reside in the ML. Arrowheads denote varicose structures along the parallel fibers that represent presynaptic sites (*12*). (**B**) Cerebellar sections as prepared in (A) were immunostained with the GFP and synapsin (top) or PSD-95 (bottom) antibodies. (**C**) Cdc20 knockdown reduced, whereas NeuroD2 and Cplx2 knockdown increased, the density of presynaptic varicosities in the cerebellar cortex in vivo ($P < 0.001$, ANOVA followed by Fisher's PLSD post hoc test, $n = 3$). Scale bars, 20 μm.

granule neurons (Fig. 2J and fig. S6F). Thus, NeuroD2 knockdown increases the density of functionally active sites of presynaptic differentiation.

In gain-of-function analyses, expression of the mutant NeuroD2 protein ND2-DBM in neurons reduced the density of presynaptic sites (Fig. 2K and fig. S7, A to C). In epistasis analyses, NeuroD2 knockdown suppressed the effect of Cdc20 knockdown on presynaptic differentiation (Fig. 2L and fig. S7, D and E). These results suggest that Cdc20-APC promotes the formation of functional presynaptic axonal sites through NeuroD2 degradation in neurons.

Among the reported NeuroD2 targets is the gene encoding Complexin II (Cplx2), a protein that modulates synaptic vesicle fusion to the presynaptic membrane in invertebrates (*9*, *10*). We asked if Cplx2 might mediate NeuroD2-dependent control of presynaptic differentiation. Knockdown of Cplx2 robustly increased the density of synapsin clusters in granule neurons, and this phenotype was reversed by expression of Cplx2 encoded by an RNAi-resistant cDNA (Cplx2-RES) but not wild-type cDNA (Cplx2-WT) (Fig. 3A and fig. S8, A and B). Cplx2 knockdown also increased the density of functionally active presynaptic axonal sites in granule neurons (Fig. 3, B to D, and fig. S8, C to F). Finally, Cplx2 knockdown increased synapsin cluster density in granule neuron parallel fiber axons in the cerebellar cortex in slices (fig. S8G). Thus, Cplx2 knockdown phenocopies the effect of NeuroD2 knockdown on presynaptic differentiation.

In epistasis analyses, expression of exogenous Cplx2 in granule neurons reduced the density of functionally active presynaptic sites induced by NeuroD2 RNAi (Fig. 3E and fig. S9, A and B). Further, although knockdown of NeuroD2 or Cplx2 each stimulated presynaptic differentiation, the combination of NeuroD2 and Cplx2 knockdown together did not additively increase the density of presynaptic sites (Fig. 3F and fig. S9, C and D). In other experiments, knockdown of Cplx2 reversed Cdc20 RNAi-induced suppression of presynaptic differentiation (Fig. 3G and fig. S9, E and F). Collectively, these results suggest that Cplx2 mediates the ability of NeuroD2 to suppress presynaptic differentiation and acts as a downstream component of the Cdc20-APC pathway in the control of presynaptic development.

We next determined the role of the Cdc20-APC ubiquitin signaling pathway in presynaptic differentiation in the developing organism. To visualize the morphogenesis of presynaptic axonal differentiation in vivo, we expressed GFP in the cerebellar cortex in rat pups using an electroporation method (*3*, *5*, *11*). These analyses revealed granule neuron cell bodies in the internal granule layer (IGL) and their parallel fiber axons in the molecular layer (ML) (Fig. 4A). Parallel fiber axons displayed varicosities along the axon (Fig. 4B), which colocalized with punctate synapsin immunoreactivity and were apposed to punctate PSD-95, a marker of postsynaptic structures (Fig. 4B). These observations indicate that parallel fiber axon varicosities represent sites of presynaptic axonal differentiation in vivo.

Using electroporation, we next induced knockdown of Cdc20, NeuroD2, or Cplx2 in rat pups. Cdc20 knockdown reduced the density of presynaptic parallel fiber varicosities in the cerebellar cortex in vivo. In contrast, knockdown of NeuroD2 or Cplx2 in rat pups increased the density of presynaptic varicosities in the cerebellar cortex (Fig. 4C and fig. S10). These results suggest that the Cdc20-APC ubiquitin signaling pathway cell-autonomously regulates presynaptic axonal differentiation in the developing brain in vivo.

We have identified a Cdc20-APC ubiquitin ligase signaling pathway that orchestrates presynaptic development and hence the establishment of neuronal circuitry in the brain (see model in fig. S11). APC function in cell cycle control has been the subject of intense scrutiny (*8*). Whereas Cdh1-APC operates in late mitosis and G1 phase of the cell cycle, Cdc20-APC controls the transition of the cell cycle through early mitosis (*8*). In the control of axon morphogenesis in postmitotic neurons, Cdh1-APC appears to control axon growth and patterning (*3*), whereas Cdc20-APC operates at a later developmental stage to promote presynaptic axonal differentiation. Thus, in an analogous manner to the temporal control of the cell cycle, the APC in concert with its two different coactivators, Cdh1 and Cdc20, appears to govern distinct temporal phases of axon differentiation in postmitotic neurons in the brain.

References and Notes

1. A. DiAntonio, L. Hicke, *Annu. Rev. Neurosci.* **27**, 223 (2004).
2. Y. Jin, C. C. Garner, *Annu. Rev. Cell Dev. Biol.* **24**, 237 (2008).
3. Y. Konishi, J. Stegmuller, T. Matsuda, S. Bonni, A. Bonni, *Science* **303**, 1026 (2004).
4. A. H. Kim *et al.*, *Cell* **136**, 322 (2009).
5. Materials and methods are available as supporting material on *Science* Online.
6. P. Chi, P. Greengard, T. A. Ryan, *Nat. Neurosci.* **4**, 1187 (2001).
7. K. I. Willig, S. O. Rizzoli, V. Westphal, R. Jahn, S. W. Hell, *Nature* **440**, 935 (2006).
8. J. M. Peters, *Nat. Rev. Mol. Cell Biol.* **7**, 644 (2006).
9. C. H. Lin *et al.*, *Proc. Natl. Acad. Sci. U.S.A.* **102**, 14877 (2005).
10. S. Huntwork, J. T. Littleton, *Nat. Neurosci.* **10**, 1235 (2007).
11. A. Shalizi *et al.*, *Science* **311**, 1012 (2006).
12. M. A. Xu-Friedman, K. M. Harris, W. G. Regehr, *J. Neurosci.* **21**, 6666 (2001).
13. We thank members of the Bonni laboratory for helpful discussions. This work was supported by NIH grants NS051255 and NS041021 (A.B.); a NSF fellowship, the Lefler Fellowship, and the Ryan Foundation (Y.Y.); a National Research Service Award Research Training grant, National Cancer Institute, and Brain Science Foundation grant (A.H.K.); the Japan Society for the Promotion of Science (T.Y.); and a Human Frontier Science Program long-term fellowship (Y.I.).

Supporting Online Material

www.sciencemag.org/cgi/content/full/326/5952/575/DC1
Materials and Methods
Figs. S1 to S13
References

1 June 2009; accepted 3 September 2009
10.1126/science.1177087

Metagenome of a Versatile Chemolithoautotroph from Expanding Oceanic Dead Zones

David A. Walsh,[1] Elena Zaikova,[1] Charles G. Howes,[1] Young C. Song,[1] Jody J. Wright,[1] Susannah G. Tringe,[2] Philippe D. Tortell,[3,4] Steven J. Hallam[1,5]*

Oxygen minimum zones, also known as oceanic "dead zones," are widespread oceanographic features currently expanding because of global warming. Although inhospitable to metazoan life, they support a cryptic microbiota whose metabolic activities affect nutrient and trace gas cycling within the global ocean. Here, we report metagenomic analyses of a ubiquitous and abundant but uncultivated oxygen minimum zone microbe (SUP05) related to chemoautotrophic gill symbionts of deep-sea clams and mussels. The SUP05 metagenome harbors a versatile repertoire of genes mediating autotrophic carbon assimilation, sulfur oxidation, and nitrate respiration responsive to a wide range of water-column redox states. Our analysis provides a genomic foundation for understanding the ecological and biogeochemical role of pelagic SUP05 in oxygen-deficient oceanic waters and its potential sensitivity to environmental changes.

Dissolved oxygen (O_2) concentration is a critical determinant of marine ecosystem structure and function. O_2 deficiency results in habitat compression and reduced productivity for aerobic organisms, with concomitant expansion of conditions favoring chemolithotrophic energy metabolism (*1*), which results in nitrogen loss and production of climate-active trace gases such as nitrous oxide (N_2O) and methane (CH_4) (*2*, *3*). Extensive oxygen minimum zones (OMZs), defined by O_2 concentrations < 20 μM, are found throughout the eastern North Pacific (ENP), eastern South Pacific (ESP), northern Indian Ocean, and southwest African shelf waters (*3*). Moreover, climate change–induced expansion and intensification of OMZs is occurring globally, with potentially deleterious effects on oceanic nitrogen cycling and carbon sequestration (*1*, *4*–*6*).

A Cdc20-APC Ubiquitin Signaling Pathway Regulates Presynaptic Differentiation

Yue Yang, Albert H. Kim, Tomoko Yamada, Bei Wu, Parizad M. Bilimoria, Yoshiho Ikeuchi, Núria de la Iglesia, Jie Shen, and Azad Bonni

Science **326** (5952), . DOI: 10.1126/science.1177087

Cdc20-APC in Synapse Formation

The E3 ubiquitin ligase Cdc20-anaphase promoting complex (Cdc20-APC) has important roles in the control of the cell division cycle. **Yang *et al.*** (p. 575) now show that Cdc20-APC also appears to be required for proper formation of synapses by developing neurons in the rat brain. When Cdc20-APC was depleted from cultured neurons or in the brains of developing rat pups, synapse formation was inhibited. The brain-enriched transcription factor NeuroD2 was shown to be a possible target of Cdc20-APC–stimulated degradation. NeuroD2 may act by promoting synthesis of Complexin II, a protein that regulates synaptic vesicle fusion.